ACS APPLIED MATERIALS & INTERFACES

www.acsami.org

Research Article

Sequential Laser-Burned Lignin and Hydrogen Evolution-Assisted Copper Electrodeposition to Manufacture Wearable Electronics

Nirmita Roy, Nida Khattak, Kat-Kim Phan, Mohammad Shakhawat Hossain, Sylvia Thomas, Manoj Ram, Michael Sheridan, Brandon Lorentz, and Arash Takshi*

Cite This: *ACS Appl. Mater. Interfaces* 2023, 15, 46571−46578

Read Online

ACCESS | Metrics & More | Article Recommendations | Supporting Information

ABSTRACT: In the contemporary world, wearable electronics and smart textiles/fabrics are galvanizing a transformation of the health care, aerospace, military, and commercial industries. However, a major challenge that exists is the manufacture of electronic circuits directly on fabrics. In this work, we addressed the issue by developing a sequential manufacturing process. First, the target fabric was coated with a customized ink containing lignin. Next, a desired circuit layout was patterned by laser burning lignin, converting it to carbon and establishing a conductive template on the fabric. At last, using an in-house-designed printer, a devised localized hydrogen evolution-assisted (HEA) copper electroplating method was applied to metalize the surface of the laser-burned lignin pattern to achieve a very low resistive circuit layout (0.103 Ω for a 1 cm long interconnect). The nanostructure and material composition of the different layers were investigated via scanning electron microscopy, energy-dispersive X-ray spectroscopy (EDX), Raman spectroscopy, and Fourier-transform infrared spectroscopy (FTIR). Monitoring the conductivity change before and after bending, rolling, stretching, washing, and adhesion tests presented remarkable mechanical stability due to the entanglement of the copper nanostructure to the fibers of the fabric. Furthermore, the HEA method was used to solder a light-emitting diode to a patterned circuit on the fabric by growing copper at the terminals, creating interconnects. The presented sequential printing method has the potential for fabricating reliable wearable electronics for various applications, particularly in medical monitoring.

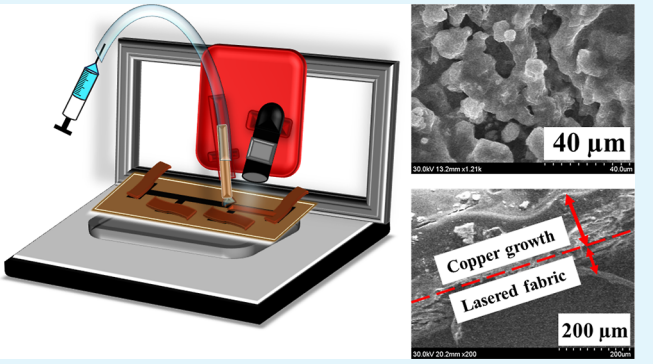

KEYWORDS: *copper, electrodeposition, laser-burned, lignin, polyester velvet fabric, smart textiles, wearable electronics*

INTRODUCTION

Wearable technologies are growing fast with the prospect of revolutionizing the health-care process for elderly people, athletes, astronauts, soldiers, etc.[1,2] While the majority of wearable electronics today are in the form of smartwatches and glasses, smart textiles/garments need to be developed for collecting health-related signals from the body of a person.[3,4] "Smart garments" refer to a broad discipline of products with extended functionality and effectiveness of common fabrics with integrated electronics into the textile for interacting with the environment or a certain user. This technology can accomplish multiple relevant functions by adding various electronics (sensors) to study, sense, and react or simply send and receive data. Wearable electronics have the potential to be widely used in various industries such as medicine to monitor the health data of patients, perform physiotherapeutic and noninvasive procedures, or perform tests such as echocardiogram (ECG) and electroencephalography (EEG).[5] They are also used in the military and aerospace industries to allow soldiers and astronauts to carry more gadgets in their vests to complete their tasks.[5]

An advanced health monitoring system often requires various sensors distributed throughout the body. Hence, interconnections between the sensors and the data collector and transmitter can go through the entire garment. In some applications, a smart suit may, also, be equipped with electrodes for electrical stimulation of muscles (i.e., physiotherapeutic feature), which requires passing a relatively large current (a few amperes) through the interconnects. Therefore, a manufacturing method is required for applying very conductive and long interconnects directly on fabrics without compromising the flexibility of the garment.

An additional but very serious challenge is related to "soldering" the electronic devices or small circuits to the conductive patterns on the textile. The conventional methods

Received: August 9, 2023
Accepted: September 11, 2023
Published: September 21, 2023

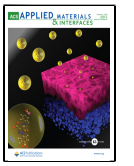

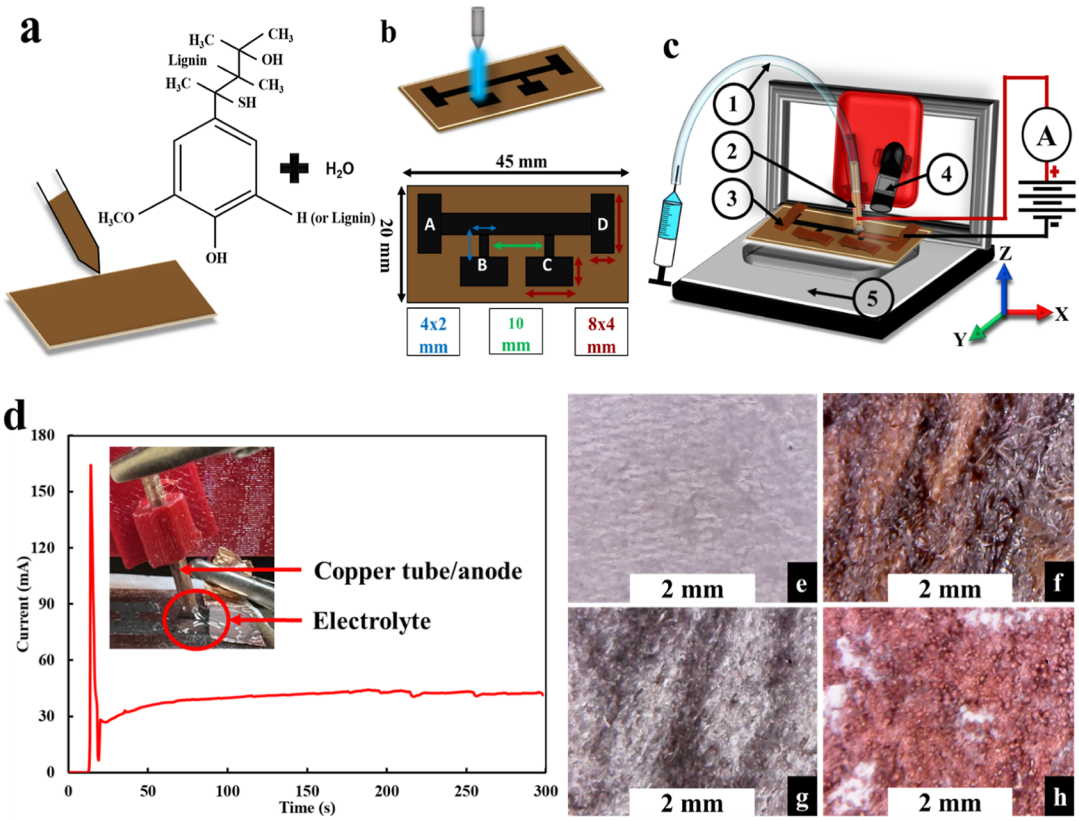

Figure 1. Sequential manufacturing process for developing wearable electronics. (a) Step 1: drop casting lignin solution on a piece of fabric, (b) step 2: laser burning a four-point probe pattern, and (c) step 3: HEA copper electrodeposition on the conductive pattern using an in-house-designed printer setup. The HEA printer has been built on (5) a motorized XYZ stage with (2) a copper tube nozzle (1) connected to a syringe pump for injection of the electrolyte. Electrical contacts to the sample were made through (3) copper tapes, and the printing process was monitored via (4) a microscope camera. (d) Current vs time during printing at 3.0 V. (inset) A picture of the nozzle during the printing. Optical microscopic images of (e) the bare polyester velvet fabric, (f) lignin coated on the fabric, (g) laser-burned lignin, and (h) an electrodeposited copper sample.

using a soldering iron or a heat flow soldering can burn fabrics. Also, conductive pastes are susceptible to mechanical stresses and break easily when the fabric is bent or stretched.[6] Aiming to integrate surface-mount devices (SMDs) into smart garments, the manufacturing method should have the capability of making patterns with a resolution compatible with the spacing between the pins of an SMD component (>1 mm) and solder directly the terminals of the device to the circuit layout on fabrics.

Wires were used in the astronauts' suits in the Apollo missions; the suit weighed about 20 kg, and it was not comfortable to wear them due to wires all over their bodies.[7] In recent years, various manufacturing methods including sewing, embroidery, weaving, knitting, coating, and printing have been practiced for integrating electronics into textiles.[8] While all these methods have been proven to be practical for specific designs or applications, each method has its limitations. Some of the methods and techniques are discussed below.

Sewing/embroidery of electrically conductive threads is a very facile and low-cost technique for acquiring wearable electronics. Conductive threads are made by coating them with metal nanoparticles (e.g., Cu, Ag, and Ni) or carbon materials [e.g., carbon nanotubes (CNTs), graphene, and activated carbon].[9−11] There are also reports of coatings with conducting polymers (CPs) and metal oxide nanoparticles such as ZnO.[12−15] In general, carbon-based threads and coatings with CPs or ZnO have low conductivity and are not suitable for long interconnects for carrying large currents. Metal-based threads have better conductivity but still a few orders of magnitude less than pure metals.[16,17] The low conductivity in the metal-based threats is due to the grain boundary effect between the conductive nanoparticles (NPs), resulting in the final sewn/embroidered pattern not being as conductive as metal interconnects in a printed circuit board (PCB). Also, making reliable connections between the device terminals and sewn conductive threads is a challenge.

Weaving and knitting of conductive threads or functionalized yarns can produce a fully integrated circuit into the textile. However, the fabrication cost is high, particularly for designing a customized smart garment. Additionally, with the use of conductive threads, the same limitations of low conductivity and soldering problems exist in these techniques.

A popular process applied by researchers is printing (screen printing or inkjet) using conductive ink made from conductive NPs. Printing is a programmable, fast, and cost-effective technique with high enough resolution for wearable electronics.[18−22] However, there are limitations to this process, mainly due to the nature of developing a conductive pattern by using dispersed NPs. To make a continuous conductive path, NPs have to be in physical contact with each other. Applied ink spreads easily on a woven structure, making it harder to produce a continuous path. Instead, a solution can be to apply highly concentrated ink (i.e., dark print) that countereffects the printing resolution.

https://doi.org/10.1021/acsami.3c11814
ACS Appl. Mater. Interfaces 2023, 15, 46571−46578

Benefiting from all the advantages of a printing method (speed, low-cost, and programable), an alternative approach is laser burning. As shown before by Chyan et al., a conductive pattern can be achieved by first coating a substrate with lignin and then laser burning it to carbonize the material.[23] The method has been used for producing conductive patterns (using a laser engraving machine) on various surfaces including fabrics.[23] However, being made of carbon, the final product is far less conductive than metals for patterning long interconnects.

Long resistive interconnects are not suitable for power-hungry wearable electronics (for therapeutic purposes or actuation). Also, smart garments with distributed sensors over the body need highly conductive interconnects to ensure a negligible voltage drop. Therefore, metallic interconnects with low resistance and the ability to carry high currents (amps level) are required. In this work, we addressed the need for a reliable fabrication method for wearable electronics through a sequential manufacturing approach. As shown in Figure 1, first the surface of the fabric is coated with an aqueous-based solution containing lignin. Then the desired pattern is applied by laser burning to produce a conductive template with the carbonized lignin. At last, a devised electrochemical method called hydrogen evolution-assisted (HEA) electroplating is used to metalize the surface of the conductive template with copper with high conductivity and the ability to carry large currents.[24−28] Copper electroplating is a common and reliable method to produce highly conductive coatings and has been used for manufacturing various electronic devices and circuits.[24] Unlike other methods using metal NPs, the electroplated surface has a continuous structure without the grain boundary effect, presenting pure metal conductivity.

For copper electroplating, a copper piece is used as the anode, and the conductive target (in this case our conductive template on fabric) is connected as the cathode. Using an aqueous-based electrolyte between the two electrodes and applying DC voltage/current, the surface of the cathode is coated with copper. However, in conventional electroplating, where the voltage difference between the anode and cathode is limited to a few hundred millivolts, the copper growth rate is limited by the mass transfer rate of ions. Equation SE1, known as the Nernst−Planck equation, shows that in the absence of electromigration (when there is an insignificant voltage drop across the bulk of the electrolyte) and lack of convection in the electrolyte, the flux of Cu^{2+} is limited by the diffusion (mass transfer).[29] Hence, for a constant DC density of J through the electrochemical cell, we can estimate the copper growth rate from[27]

$$\text{deposition rate} = (JM_w)/nF\rho \quad (1)$$

where M_w is the atomic copper weight (63.5 g mol^{-1}), F (96,485 C mol^{-1}) is the Faraday constant, n (=2) is the oxidation state of copper, and ρ is the copper density (8.63 g cm^{-3}). A typical current density of 20 mA cm^{-2} implies ∼7.6 nm s^{-1} deposition rate, which is too slow for printing applications.[27] Obviously, increasing the current increases the rate linearly. Considering the cell resistance, increasing current forces the voltage. However, when the cell voltage exceeds 1.23 V, concurrent to copper deposition, water electrolysis occurs, which is a totally different mode of electroplating called the HEA method. In this mode, due to hydrogen bubbling near the cathode, electrolyte convection forces beyond diffusion, resulting in a faster growth rate.[27] Also, the presence of bubbles results in the formation of a porous structure with relatively lower ρ values than compact copper. The combination of employing convection and producing a porous structure in the HEA mode allows us to reach an incredibly fast growth rate. In fact, we have shown that the HEA electroplating method can be used for fast printing copper on fabrics reaching a lateral copper growth rate exceeding 370 $\mu m\ s^{-1}$.[25] Although in general, HEA electroplated layer integrity is not as strong as compact copper structures, the final pattern is integrated into the fabric with remarkable stability due to the nanostructures of the grown copper layer being diffused into the fiber of the fabric.[24,26] While our earlier works prove the feasibility of using HEA for wearable electronics to produce high-quality and reliable results for long interconnects, as explained in the Supporting Information, the resistive nature of the template requires localized electroplating. Hence, in this work, an electrochemical printer machine (Figures 1c and S2) has been designed. The quality of different layers during the manufacturing steps has been studied and reported. Although laser burning of lignin to produce a conductive pattern on fabrics is not a new technique,[30,31] the sequential process presented in this work and the designed HEA electroplating printer prove to be cost-effective and produce conductive patterns that can be used for long and low-resistance interconnections between distributed sensors on a smart garment. Further details about HEA electroplating are explained in Section S2 and in other publications.[32−35]

RESULTS AND DISCUSSION

Manufacturing Results. Figure 1 shows the three steps of the manufacturing process: (1) drop casting the lignin solution on a piece of fabric, (2) applying the desired conductive pattern by laser burning the lignin coating, and (3) electroplating the surface of the conductive pattern using the designed printer machine. The pictures of the laser engraving system and the actual electrochemical printer machine are presented in Figure S2 in the Supporting Information. To measure the conductivity with the four-probe method, a pattern shown in Figure 1b were laser burned and later electroplated. A picture of the sample is shown in Figure S3.

The HEA printer was designed with a copper tube as the nozzle and anode (Figure 1c, ②). The nozzle was mounted on a motorized XYZ stage ⑤ where the fabric sample with the laser-burned template was placed. Using a piece of copper tape at a corner of the template ③, the pattern was connected as the cathode to the external voltage source. The nozzle was connected to a syringe pump with a flexible tube ①. Adjusting the speed of the syringe pump, a droplet of the electrolyte can be formed at the tip of the nozzle (Figure 1d, inset) while bridging between the anode and cathode. For printing copper, the nozzle was moved near the copper tape that made contact with the template. The HEA electroplating was started after application of 3.0 V in the presence of the electrolyte. It should be noted that as shown in Figure S1, due to the resistive nature of the template, first it is required to have a localized electrochemical printing with a short distance between the anode and cathode contact to control the growth rate. Also, a voltage larger than 1.23 V must be applied to compensate for the voltage drop (ΔVr in Figure S1) in the series resistance. Changing the voltage is expected to affect the quality and the speed of printing, which will be further studied in our future works. The copper growth was monitored via an installed

https://doi.org/10.1021/acsami.3c11814
ACS Appl. Mater. Interfaces 2023, 15, 46571−46578

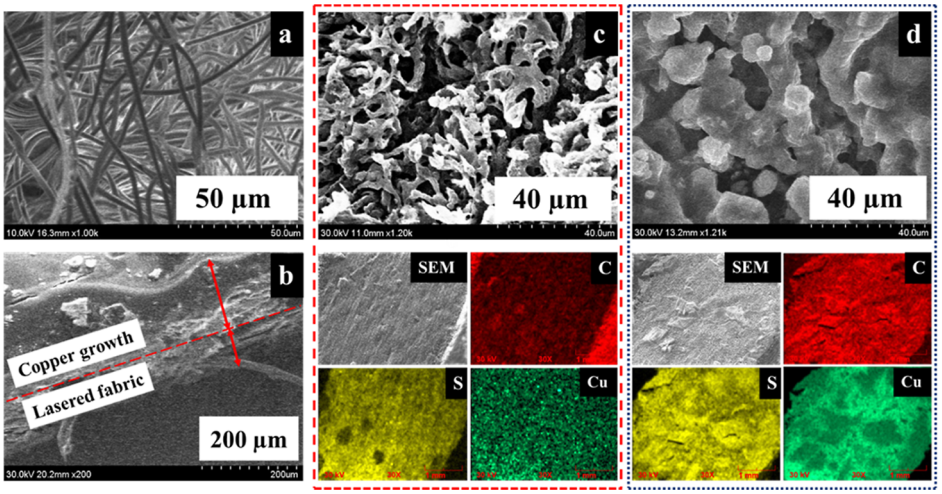

Figure 2. (a) SEM image of the polyester velvet fabric. (b) Cross-section SEM image of the fabric with the electrodeposited copper. (c) Top—SEM image of the lasered lignin; bottom—EDX mapping images. (d) Top—SEM image of the electrodeposited copper on the fabric; bottom—EDX mapping images of electrodeposited copper.

microscope camera on the printer head (Figure 1c, ④). Using the console of the XYZ stage, the nozzle hovered over the pattern as the copper was growing. The speed of moving the sample was adjusted manually by the operator based on the live image of the process through the microscope camera. The HEA electroplating current was recorded and is shown in Figure 1d. During the first 12 s, the current remained at zero when the droplet was not in touch with the sample yet. At the 13th second, when the electrolyte made contact with the fabric, the current spiked up to 162 mA. Since the power source (3.0 V) was already applied between the anode and cathode before the electrolyte bridges between the two electrodes, at first, the double layer charges were formed on the electrodes, which resulted in the spiked current. Shortly after the formation of the double layer, the current dropped to a lower value at which the HEA process started. In about 2−3 s, as soon as the copper started to grow on the laser-burned lignin, the current reached ∼28 mA. Moving the nozzle manually over the sample, the current fluctuated between 32 and 43 mA during the printing process.

The recorded video process, which shows copper growth concurrent with hydrogen evolution is available in the Supporting Information in Section S8. It should be noted that due to the nature of electroplating that grows only on conductive surfaces, the feature size was determined by the laser burning resolution, not the size of the nozzle or the electrolyte meniscus. However, if the nozzle was kept at a location for a longer time, as the copper layer thickness increases, lateral growth would be expected too. In the designed printing system when the nozzle is moving, the copper layer thickness and the lateral growth are limited, allowing us to coat only on the conductive template. The conducted experiment showed the feasibility of printing copper with an average speed of 0.7 mm s^{-1}. The optical images in Figure 1e−h show that relatively uniform coatings of lignin, laser-burned pattern, and deposited copper layers were achieved. After each step, samples were dried before the characterization.

Characterization Results. To perceive the structures of the samples and analyze their surfaces, scanning electron microscopy (SEM) and energy-dispersive X-ray (EDX) spectroscopy methods were used. The SEM method was used to evaluate the surface morphology at different stages of the experiment, as shown in Figure 2. Figure 2a shows the SEM image of the bare velvet fabric as it was purchased. Figure 2c,d shows the structures of the fabric after laser burning of lignin and copper deposition, respectively. Clearly, the fibrous structure of the fabric was significantly changed after laser burning. Also, the HEA electroplated copper presented porous nanostructures while forming a continuous structure. Figure 2b exhibits the cross-section SEM image of the fabric and electrodeposited copper showing an integrated structure of the copper layer to the fabric.

The composition of the conductive template before and after the electroplating was further studied with EDX, as shown in Figure 2c,d (bottom). The mapping images verify a uniform distribution of different elements on the surface.

Table 1 establishes the elements along with their concentrations in weight % unit for each EDX analysis performed.

Table 1. EDX Spectrum

	concentrations (wt %)	
element name	after laser- burning lignin	after copper electrodeposition
C	69.725	39.433
S	16.636	16.023
Cu	1.278	43.376

The data in Table 1 indicate that the laser-burned lignin had the highest concentration of carbon (69.725 wt %) followed by sulfur with 16.636 wt % and a small amount of copper. In contrast, after the electroplating, copper became the dominant element with a concentration of 43.376 wt % followed by carbon with 39.433 wt % and sulfur with 16.023 wt %. The kraft lignin purchased from Sigma-Aldrich (CAS no: 8068-05-1) has about 4% sulfur impurities as mentioned in its datasheet, which is why the EDX spectrum detected sulfur in the lasered lignin sample. The presence of sulfur from the electrolyte (containing $CuSO_4$ and H_2SO_4) is also detected in the electrodeposited copper sample. The entire EDX spectrum and element mapping are provided in the Supporting Information (Figures S4 and S5 and Table S1).

https://doi.org/10.1021/acsami.3c11814
ACS Appl. Mater. Interfaces 2023, 15, 46571−46578

To understand the transformation of lignin to a conductive material after laser burning, the molecular structure of the layers after lasering the lignin was further investigated through Raman and Fourier-transform infrared (FTIR) spectroscopies.

As shown in Figure 3a, the Raman spectra for the laser-burned lignin represent two dominating peaks at 1354 and

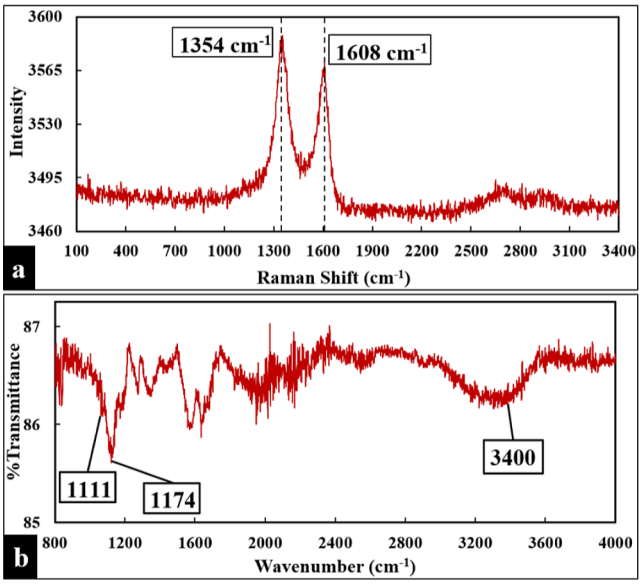

Figure 3. (a) Raman and (b) FTIR spectra of the laser-burned lignin sample. FTIR data cover wavenumbers of 4000 to 800 cm^{-1}.

1608 cm^{-1}. The peak at 1354 cm^{-1} is influenced by the defects in lignin resulting in a D peak, where D represents a disorder in graphene, whereas the peak at 1608 cm^{-1} is influenced by the planar configuration by sp^2-bonded carbon constituting graphene as a part of lignin resulting in the G (graphite) peak.[36−38] This shows that laser-burned lignin can induce it to produce a primary source of graphene/graphite.[23,36,39]

To correlate our results, we then performed FTIR spectroscopy in the attenuated total reflectance (ATR) mode to attain information associated with the absence or presence of specific functional groups for our fabric concerning the laser-burned lignin samples, as shown in Figure 3b. The corresponding group and compound class and the respective bands are discussed below. Based on previous studies,[40−43] the FTIR data were analyzed. The slight bends at around 3400 cm^{-1} show some moisture (O−H stretching resulting in the formation of H-bonds) in the samples. The significant band peak appearing at 1174 cm^{-1} relates to the attributes of amorphous cellulose.[44] The 1111 cm^{-1} peak corresponds to the C−H in the plane deformation relating to the presence of syringyl.[43]

Stability and Flexibility Testing Results. Since the conductivity of the produced pattern is of the greatest interest in this work, we used the specifically designed pattern in Figure 1b to do the four-point probe conductivity measurement before and after electroplating. Measurements were conducted by applying a constant current through the two outer pads (A and D in Figure 1b) and reading the voltage between the two inner pads (B and C). The measured resistance was found to be 168 Ω for the lignin-burned template, while it dropped to 0.103 Ω after electroplating. Considering the length and width of the strip between connections to pads B and C and the measured thickness of the layers from Figure 2b, the conductivity was estimated to be 5.95 S cm^{-1} for the carbonized lignin and improved by 3 orders of magnitude after the metallization reaching the conductivity of 1.28×10^3 S cm^{-1}. Although the achieved conductivity is still lower than that in pure copper (5.9×10^5 S cm^{-1}), we believe the conductivity can be enhanced by adjusting the speed of printing and the HEA electroplating voltage to form a more uniform coating. Nevertheless, reducing the resistance of the conductive pattern from 168 to 0.103 Ω approves the feasibility of manufacturing low-resistive interconnects on fabrics. To assess the ability of the conductive pattern for carrying large currents, a DC as high as 0.2 A was passed through the conductive strip. The sample's resistance did not change after the high-current test, confirming the feasibility of using the sequential fabrication method for high-current wearable applications.

The mechanical stability and flexibility of the conductive pattern were tested in a series of experiments. A 3D-printed cylinder of 1.27 cm diameter was employed to roll on the samples back and forth 10 times to test for any change in conductivity measurements, resulting in no change in resistance values. After performing the rolling process, we utilized two different 3D-printed semicylinder structures with diameters of 2.54 and 3.81 cm to bend the samples while simultaneously recording the conductivity data. The experiment showed zero change in the four-probe measured resistance. Figure S6 shows the sample under the test, presenting remarkable flexibility without losing its conductivity. It is believed that the porous copper structure shown in Figure 2d promotes the flexibility of the copper layer with high stability and without losing conductivity under the bending conditions.

As washability is an important feature of clothes, we tested the sample by sinking it in a beaker filled with deionized (DI) water for 5 min and drying them in air. We remeasured the resistance after the sample was dried only to find that the resistance increased by ∼0.03 Ω. Visual inspection with a microscope camera did not show any specific changes in the copper layer. However, the exposure to water had likely accelerated the oxidation of copper underneath the surface, affecting the conductivity. In our future works, to address stability, we consider coating a passivation layer over the interconnects.

Additionally, as shown in Figure S7, adhesion tests were conducted by applying Scotch 3M Satin Finish Gift Wrap Tape over each electroplated sample and adding 1.4 kg weight on the samples for 2 min, after which we ripped the tapes in two different motions−sharp and slow, as instructed by the "Adhesion by Tape Test" standard (ASTM D3359-23), to compare how much copper would come off the fabric and how that would affect the conductivity data. Ripping the tapes both swiftly and slowly did not take off any of the copper deposited on the samples and also did not affect the resistance of the samples, proving again the outstanding adhesion of the copper layer. The sample was also tested for hardness using a portable Shore D durometer. The hardness measurement was done at three different testing points, and the average of the readings was calculated. As Table S2 shows, the process of laser burning of lignin and electroplating of copper did not make any significant change in the hardness of the sample.

Furthermore, we used a digital push−pull force gauge dynamometer to test the effect of stress on the sample with

https://doi.org/10.1021/acsami.3c11814
ACS Appl. Mater. Interfaces 2023, 15, 46571−46578

respect to resistance. As shown in Figure S8, the samples were placed in between two flat-nose plier heads tightly and stretched until they were ripped to measure conductivity data and force required. The change in resistance with respect to the stress applied is given in Figure 4. The results show that the

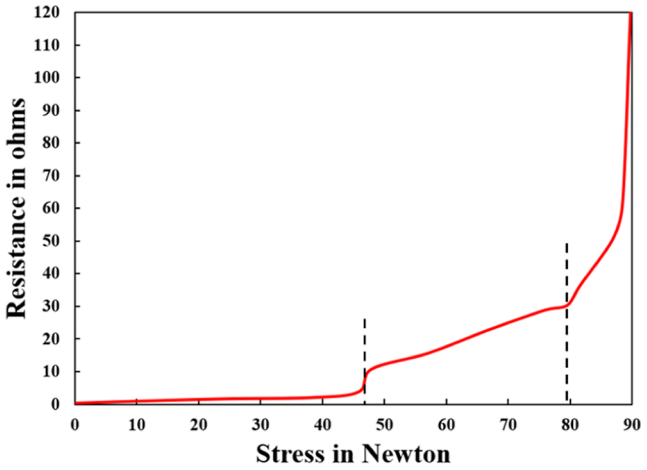

Figure 4. Change in resistance with respect to stress.

resistance was increased almost linearly up to 47 N force at which the resistance showed a sudden increase when the conductive part starts to fracture. Further stretching caused damage to the fabric around 79 N force when it started to rip out.

Room Temperature Soldering of a Light-Emitting Diode. The sequential manufacturing method was further applied for integrating an SMD light-emitting diode (LED) into a simple circuit layout. First, two conductive strips (4 mm × 15 mm) with a gap of 1 mm were laser burned to develop the conductive template. Using a dot of hot glue, an LED was glued in the middle of the laser-burned fabric right before electrodeposition. Once it dried, we carried out our process to grow copper on the lasered pattern, reaching the LED terminals. To "solder," the nozzle was kept above the junction for an extended time (~20 s) to allow the copper to grow vertically. As the process was monitored through the microscope camera, the nozzle was moved manually along the *Z* direction to grow copper over the terminals of the device, forming a continuous copper structure connecting the device to the electroplated interconnect. Figure 5 shows the soldered LED. We tested the electrical connections by turning on and off the LED when it was connected to an external Arduino board (Figure 5c,d).

This sequential process of laser burning of lignin and HEA electrodeposition of copper directly on fabrics shows promising results in terms of high conductivity, stability, and flexibility, which can address the needs for designing power-hungry wearable electronics and/or distributed sensor designs for health monitoring. The metallic pattern can provide PCB-quality interconnects for smart garments. Also, the process is a cost-effective and low-temperature method for solder sensors and other electronic devices to produce wearable electronics with more functionality. To achieve higher quality, an automated system for the HEA printer is planned to adjust the speed of printing, electrochemical voltage, and electrolyte injection rate (through the syringe pump). In the new design, the printer will be equipped with a second nozzle (e.g., inkjet)

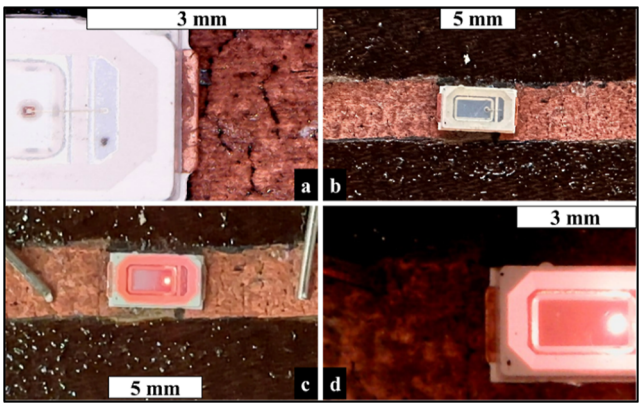

Figure 5. Optical microscopic images of (a) copper junction, (b) copper electrodeposition, (c) LED powered up by the Arduino board, and (d) closer image of the powered-up LED.

to print an insulating material over the printed copper to passivate the metal and protect it against oxidation.

METHODS

Materials. $CuSO_4$ (CAS no: 7758-98-7), H_2SO_4 (CAS no: 7664-93-9), and Kraft Lignin (structure in Figure 1a) in the form of a brown to black powder with a low sulfonate content (CAS no: 8068-05-1) were purchased from Sigma-Aldrich. A white microfiber microsuede, 100% woven polyester velvet fabric, was purchased from KOVI Fabrics (pattern no: K4175) to be used for all research conducted.

Preparation of the Lignin Solution and HEA Electrolyte. Two grams of lignin were added to 10 mL of DI water and stirred for about 5 min until all the lignin dissolved. We found the best results by depositing 260 μL of the solution on the velvet fabric with dimensions of 45 mm length × 20 mm width by pipetting it and drying it for 24 h (the process is shown in Figure 1a). The HEA electrolyte was an aqueous solution prepared with 0.47 M $CuSO_4$ and 1.5 M H_2SO_4 mixed with 10 mL of DI water for 5 min until thoroughly dissolved.[26]

Laser Burning Lignin and Electrodepositing Copper. To study the four-probe conductivity, a pattern with four pads A, B, C, and D, each measuring 8 mm × 4 mm and spaced at every 10 mm, was designed with LaserDRW software (pattern with dimensions shown in Figure 1b). The lignin-coated fabric after drying was placed in an OMTech 40W CO_2 Laser Engraver Machine (model no: SH-G3020) to laser burn the four-probe design. The laser power was set at 5%, and the pattern was rasterized twice. After the carbonization of lignin, the sample was placed in an in-house-designed copper electroplating printer to metalize the surface of the conductive pattern (Figure 1c). The syringe (5 mL) was filled with the electrolyte and placed into the syringe pump at a rate of 12 mL h^{-1}. The nozzle was a copper tube of 2 mm diameter (Figure 1c, ②) that served as the anode and was mounted on a motorized XYZ stage (model: Genmitsu CNC 3018-PRO router kit GRBL Control 3 axis machine, XYZ working area 300 × 180 × 45 mm, as shown in Figure 1c, ⑤). For electroplating, the laser-burned template on the fabric was placed on the printer stage. Using a piece of copper tape, one end of the laser-burned track (starting point) was connected to a potentiostat (Princeton Applied Research: model VersaSTAT 4) as the cathode, using the copper tube as the anode. A constant voltage of 3.0 V was applied to the cathode with respect to the anode while recording the electrochemical current via the potentiostat. The motion of the nozzle was controlled manually via the electronic console of the XYZ stage. The process of printing is explained in the Results and Discussion. The sequential fabrication steps and the structure of the devised electroplating printer are presented in Figures 1 and S2 in the Supporting Information.

Characterization. A Hitachi SU-70 high-resolution field emission SEM instrument was used for imaging and collecting EDX data.

https://doi.org/10.1021/acsami.3c11814
ACS Appl. Mater. Interfaces 2023, 15, 46571−46578

Raman spectroscopy was conducted by using the Jasco NRS-4500 series laser probe spectroscopy system. We performed FTIR spectroscopy in ATR mode on a PerkinElmer 100 spectrometer. A Keithley 2602A SourceMeter instrument was used for four-point probe conductivity measurements. For stretching samples, we used the Ailigu ZP series digital push−pull force gauge dynamometer tester.

CONCLUSIONS

Implementing the laser-burning process to velvet fabric with the help of lignin and electrodepositing copper on the lasered pattern can be advantageous for various applications, to achieve longer interconnects and embedding multiple devices or sensors under low resistance. Laser-burning the coated lignin on the fabric converted the nonconductive lignin into a higher-quality graphene/graphite. This process can be a good solution in terms of stability and flexibility. The copper electrodeposition process with the designed printing machine shows promising results of uniform copper growth at a faster rate of speed than conventional electroplating, providing futuristic developments for state-of-the-art wearable electronics.

ASSOCIATED CONTENT

Supporting Information

The Supporting Information is available free of charge at https://pubs.acs.org/doi/10.1021/acsami.3c11814.

Understanding of HEA electroplating and additional experimental details and their results, including pictures of the experimental setup (PDF)

Copper electrodeposition by the HEA electroplating method (MOV)

AUTHOR INFORMATION

Corresponding Author

Arash Takshi − *University of South Florida, Tampa, Florida 33620, United States;* orcid.org/0000-0002-4582-8077; Email: atakshi@usf.edu

Authors

Nirmita Roy − *University of South Florida, Tampa, Florida 33620, United States;* orcid.org/0000-0001-5932-2870

Nida Khattak − *University of South Florida, Tampa, Florida 33620, United States*

Kat-Kim Phan − *University of South Florida, Tampa, Florida 33620, United States*

Mohammad Shakhawat Hossain − *University of South Florida, Tampa, Florida 33620, United States*

Sylvia Thomas − *University of South Florida, Tampa, Florida 33620, United States*

Manoj Ram − *PolyMaterialsApp, Tampa, Florida 33612, United States*

Michael Sheridan − *PolyMaterialsApp, Tampa, Florida 33612, United States*

Brandon Lorentz − *PolyMaterialsApp, Tampa, Florida 33612, United States*

Complete contact information is available at: https://pubs.acs.org/10.1021/acsami.3c11814

Author Contributions

A.T. designed the experiments and advised the project. S.T. was the advisor of the funded project. N.R. and N.K. executed the experiments and collected the data. K.-K.P. worked on the design of the electrodeposition printer. M.S.H. carried out the SEM, EDX, and Raman analyses. M.R., M.S., and B.L. helped analyze the FTIR data. N.R. analyzed and acquired the experimental data for Raman, FTIR, and other tests performed.

Notes

The authors declare no competing financial interest.

ACKNOWLEDGMENTS

This work was financially supported by the National Science Foundation through NSF 1953089.

REFERENCES

(1) Tao, X. *Wearable Electronics and Photonics*; Elsevier, 2005.

(2) Ferreira, J. J.; Fernandes, C. I.; Rammal, H. G.; Veiga, P. M. Wearable Technology and Consumer Interaction: A systematic review and research agenda. *Comput. Hum. Behav.* **2021**, *118*, 106710.

(3) Nugroho, J. A Conceptual Framework for designing Wearable Technology. *Faculty of Design, Architecture & Building*; University of Technology—Sydney, 2013.

(4) Kurwa, M.; Mohammed, A.; Liu, W. *Wearable Technology, Fashioning the Future*; Flextronics. Retrieved May 13, 2014, 2008.

(5) Stoppa, M.; Chiolerio, A. Wearable Electronics and Smart Textiles: A critical review. *sensors* **2014**, *14* (7), 11957−11992.

(6) Benešová, A.; Hirman, M.; Hlína, J.; Tupa, J.; Steiner, F.; Řeboun, J. Optimization of Contacting Technological Process on Printed Conductive Pattern for Wearable Electronics. *2020 43rd International Spring Seminar on Electronics Technology (ISSE)*, 2020; pp 1−7. 14−15 May 2020.

(7) Bellisle, R.; Bjune, C.; Newman, D. Considerations for Wearable Sensors to monitor Physical performance during Spaceflight Intravehicular activities. *2020 42nd Annual International Conference of the IEEE Engineering in Medicine & Biology Society (EMBC)*; IEEE, 2020; pp 4160−4164.

(8) Nasiri, S.; Khosravani, M. R. Progress and Challenges in Fabrication of Wearable Sensors for Health Monitoring. *Sens. Actuators, A* **2020**, *312*, 112105.

(9) Rahimi, R.; Yu, W.; Parupudi, T.; Ochoa, M.; Ziaie, B. A low-cost Fabrication Technique for Direct Sewing Stretchable Interconnections for Wearable Electronics. *2015 Transducers—2015 18th International Conference on Solid-State Sensors, Actuators and Microsystems (TRANSDUCERS)*, 2015; pp 1350−1353, 21−25 June 2015.

(10) Ning, C.; Tian, L.; Zhao, X.; Xiang, S.; Tang, Y.; Liang, E.; Mao, Y. Washable Textile-Structured Single-Electrode Triboelectric Nanogenerator for self-powered Wearable Electronics. *J. Mater. Chem. A* **2018**, *6* (39), 19143−19150.

(11) Tao, X.; Koncar, V.; Huang, T.-H.; Shen, C.-L.; Ko, Y.-C.; Jou, G.-T. How to Make Reliable, Washable, and Wearable Textronic Devices. *Sensors* **2017**, *17* (4), 673.

(12) Li, Y.; Peng, H.; Peng, Y.; Zhou, J.; Zhang, J. Thermoplastic and Electrically Conductive Fibers for Highly Stretchable and Sensitive Strain Sensors. *ACS Appl. Polym. Mater.* **2022**, *4* (12), 8795−8802.

(13) Hu, J.; Gao, B.; Qi, Q.; Zuo, Z.; Yan, K.; Hou, S.; Zou, D. Flexible and Conductive Polymer Threads for Efficient Fiber-Shaped Supercapacitors via Vapor Copolymerization. *ACS Omega* **2022**, *7* (36), 31628−31637.

(14) Zhu, C.; Wu, J.; Yan, J.; Liu, X. Advanced Fiber Materials for Wearable Electronics. *Advanced Fiber Materials* **2023**, *5* (1), 12−35.

(15) Li, X.; Chen, S.; Peng, Y.; Zheng, Z.; Li, J.; Zhong, F. Materials, Preparation Strategies, and Wearable Sensor Applications of Conductive Fibers: A Review. *Sensors* **2022**, *22* (8), 3028.

(16) Kareri, T.; Yadav, R. L.; Takshi, A. Image Processing Analysis of Supercapacitors with Twisted Fiber structures and a Gel Electrolyte. *J. Appl. Electrochem.* **2022**, *52* (1), 139−148.

(17) Kareri, T.; Hossain, M. S.; Ram, M. K.; Takshi, A. J. A Flexible Fiber-shaped Hybrid Cell with a Photoactive Gel Electrolyte for

Concurrent Solar Energy Harvesting and Charge Storage. *Int. J. Energy Res.* **2022**, *46* (12), 17084−17095.
(18) Yan, K.; Li, J.; Pan, L. J.; Shi, Y. Inkjet Printing for Flexible and Wearable Electronics. *APL Mater.* **2020**, *8*, 120705.
(19) Gao, M.; Li, L.; Song, Y. Inkjet Printing Wearable Electronic devices. *J. Mater. Chem. C* **2017**, *5* (12), 2971−2993.
(20) Delibozov, N. G.; Spasova, M. L. Inkjet-Printing in Development of Flexible and Wearable Sensing Electronics. *2019 IEEE XXVIII International Scientific Conference Electronics (ET)*; IEEE, 2019; pp 1−4.
(21) Beedasy, V.; Smith, P. J. Printed Electronics as Prepared by Inkjet Printing. *Materials* **2020**, *13* (3), 704.
(22) Carey, T.; Cacovich, S.; Divitini, G.; Ren, J.; Mansouri, A.; Kim, J.; Wang, C.; Ducati, C.; Sordan, R.; Torrisi, F. Fully Inkjet-Printed Two-Dimensional Material Field-Effect Heterojunctions for Wearable and Textile Electronics. *Nat. Commun.* **2017**, *8*, 1202.
(23) Chyan, Y.; Ye, R.; Li, Y.; Singh, S. P.; Arnusch, C. J.; Tour, J. M. Laser-Induced Graphene by Multiple Lasing: Toward Electronics on Cloth, Paper, and Food. *ACS Nano* **2018**, *12* (3), 2176−2183.
(24) Rosa-Ortiz, S. M.; Phan, K.-K.; Khattak, N.; Thomas, S. W.; Takshi, A. Hydrogen Evolution Assisted Cyclic Electroplating for Lateral Copper Growth in Wearable Electronics. *J. Electroanal. Chem.* **2021**, *902*, 115796.
(25) Rosa-Ortiz, S. M.; Takshi, A.; Thomas, S. Advances in Lateral Copper Electroplated Metallic Tracks—Production and Applications by using Hydrogen Evolution-Assisted Electroplating. *MRS Advances* **2021**, *6*, 654−658.
(26) Rosa-Ortiz, S. M.; Takshi, A. In Copper Electrodeposition by Hydrogen Evolution Assisted Electroplating (HEA) for Wearable Electronics. *2020 Pan Pacific Microelectronics Symposium (Pan Pacific)*, 2020; pp 1−5. 10−13 Feb 2020.
(27) Rosa-Ortiz, S. M.; Khorramshahi, F.; Takshi, A. Study the Impact of CuSO4 and H2SO4 Concentrations on Lateral Growth of Hydrogen Evolution Assisted Copper Electroplating. *J. Appl. Electrochem.* **2019**, *49* (12), 1203−1210.
(28) Rosa-Ortiz, S. M.; Kadari, K. K.; Takshi, A. J. M. A. Low Temperature Soldering Surface-Mount Electronic Components with Hydrogen Assisted Copper Electroplating. *MRS Advances* **2018**, *3*, 963−968.
(29) Bard, A. J.; Faulkner, L. R. *Electrochemical Methods: Fundamentals and Applications*, 2nd ed.; Wiley, 2001; pp 146−153.
(30) Luo, Y.; Miao, Y.; Wang, H.; Dong, K.; Hou, L.; Xu, Y.; Chen, W.; Zhang, Y.; Zhang, Y.; Fan, W. Laser-Induced Janus Graphene/poly (p-phenylene benzobisoxazole) Fabrics with Intrinsic Flame Retardancy as Flexible Sensors and Breathable Electrodes for Fire-Fighting Field. *Nano Res.* **2023**, *16* (5), 7600−7608.
(31) Tao, L.-Q.; Tian, H.; Liu, Y.; Ju, Z.-Y.; Pang, Y.; Chen, Y.-Q.; Wang, D.-Y.; Tian, X.-G.; Yan, J.-C.; Deng, N.-Q.; Yang, Y.; Ren, T.-L. An Intelligent Artificial Throat with Sound-Sensing ability based on Laser Induced Graphene. *Nat. Commun.* **2017**, *8* (1), 14579.
(32) Shin, H.-C.; Dong, J.; Liu, M. Nanoporous Structures Prepared by an Electrochemical Deposition Process. *Adv. Mater.* **2003**, *15* (19), 1610−1614.
(33) Nikolić, N.; Popov, K. I.; Pavlović, L.; Pavlović, M. The Effect of Hydrogen Co-deposition on the Morphology of Copper Electrodeposits. I. The Concept of Effective Overpotential. *J. Electroanal. Chem.* **2006**, *588* (1), 88−98.
(34) Plowman, B. J.; Jones, L. A.; Bhargava, S. K. Building with Bubbles: the formation of High Surface area Honeycomb-like Films via Hydrogen Bubble Templated Electrodeposition. *Chem. Commun.* **2015**, *51* (21), 4331−4346.
(35) Wang, M.; Yu, X.; Wang, Z.; Gong, X.; Guo, Z.; Dai, L. Hierarchically 3D Porous Films Electrochemically constructed on Gas−Liquid−Solid Three-Phase Interface for Energy Application. *J. Mater. Chem. A* **2017**, *5* (20), 9488−9513.
(36) Mahmood, F.; Zhang, H.; Lin, J.; Wan, C. Laser-Induced Graphene Derived from Kraft Lignin for Flexible Supercapacitors. *ACS Omega* **2020**, *5* (24), 14611−14618.
(37) Wang, B.; Shi, T.; Zhang, Y.; Chen, C.; Li, Q.; Fan, Y. Lignin-based Highly Sensitive Flexible Pressure Sensor for Wearable Electronics. *J. Mater. Chem. C* **2018**, *6* (24), 6423−6428.
(38) Tuschel, D. Raman Spectroscopy of Oil Shale. *Spectroscopy* **2013**, *28*, 20.
(39) Ye, R.; James, D. K.; Tour, J. M. Laser-Induced Graphene. *Acc. Chem. Res.* **2018**, *51* (7), 1609−1620.
(40) Mohamad Ibrahim, M. N.; Zakaria, N.; Sipaut, C. S.; Sulaiman, O.; Hashim, R. Chemical and Thermal Properties of Lignins from Oil Palm Biomass as a Substitute for Phenol in a Phenol Formaldehyde Resin Production. *Carbohydr. Polym.* **2011**, *86* (1), 112−119.
(41) Hergert, H. L. Infrared Spectra of Lignin and Related Compounds. II. Conifer Lignin and Model Compounds1,2. *J. Org. Chem.* **1960**, *25* (3), 405−413.
(42) Faix, O. Classification of Lignins from Different Botanical Origins by FT-IR Spectroscopy. *Holzforschung* **1991**, *45* (s1), 21−28.
(43) Ibrahim, M. N. M.; Iqbal, A.; Shen, C. C.; Bhawani, S. A.; Adam, F. Synthesis of Lignin based Composites of TiO2 for potential application as Radical Scavengers in Sunscreen Formulation. *BMC Chemistry* **2019**, *13* (1), 17.
(44) de Souza, A. G.; Junqueira, M. T.; de Lima, G. F.; Rangari, V. K.; Rosa, D. S. A New Proposal of Preparation of Different Polymorphs of Nanocellulose from Eucalyptus citriodora. *J. Polym. Environ.* **2020**, *28* (4), 1150−1159.

https://doi.org/10.1021/acsami.3c11814
ACS Appl. Mater. Interfaces 2023, 15, 46571−46578